

## Diffusion-Limited Acid–Base Nonexponential Dynamics

Boiko Cohen and Dan Huppert\*

School of Chemistry, Raymond and Beverly Sackler Faculty of Exact Sciences, Tel-Aviv University, Ramat-Aviv, Tel-Aviv 69978, Israel

Noam Agmon

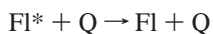
The Fritz Haber Research Center, Department of Physical Chemistry, The Hebrew University, Jerusalem 91904, Israel

Received: February 22, 2001; In Final Form: May 14, 2001

Using time-resolved fluorescence, we have measured the direct proton transfer reaction between a photoacid, 2-naphthol-6-sulfonate, and a base, acetate anion, in water–glycerol mixtures. The reaction shows clear evidence for irreversible diffusion-controlled reactivity in agreement with the Smoluchowski model. As the solution viscosity increases, from about 1 cP (neat water) to 40 cP at 0.4 mole fraction of glycerol, the initial ROH\* fluorescence decay becomes increasingly nonexponential, providing clear evidence for the transient regime of the Smoluchowski model for a real chemical reaction.

### Introduction

The dynamics of fast bimolecular reactions in solution have, for a long time, been a subject of interest to both experimentalists and theoreticians. The kinetics of many physical, chemical and biological processes are influenced by diffusion.<sup>1</sup> Electron and hole trapping processes in semiconductors;<sup>2</sup> fluorescence quenching;<sup>3–8</sup> excimer formation;<sup>9,10</sup> acid–base reactions;<sup>11–15</sup> ion association–dissociation;<sup>16</sup> electron-transfer reactions;<sup>17</sup> and the dynamics of proteins, enzymes, and membranes<sup>18,19</sup> are common examples of such processes. Several of these processes occur in the excited state.<sup>11–15,20,21</sup> Bimolecular irreversible diffusion influenced reactions between donors and acceptors, in the pseudo-unimolecular limit when one reactant (say, the acceptor) is in excess, are the subject of the celebrated “Smoluchowski theory”.<sup>22–27</sup> In the limit that the donor is static, this theory is exact.<sup>25,27</sup> It is also an excellent approximation when both donor and acceptors move.<sup>28,29</sup> The initial decay is faster than exponential due to the excess of acceptors at close proximity to a given donor. As this density approaches its steady-state limit, the reaction becomes exponential, with the ubiquitous diffusion-control rate coefficient  $k_D$ . This theory has been applied predominantly to fluorescence quenching<sup>3–8</sup> between an excited fluorophore (Fl\*) and quencher molecules (Q)



Yet it proved difficult to find conclusive experimental evidence for the predicted fluorescence quenching kinetics in the non-exponential time regime.<sup>8</sup>

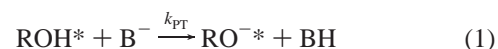
Another type of reaction that can be treated by diffusion formalism is reversible proton transfer to solvent (PTTS) from an excited organic photoacid (ROH\*), and the subsequent

geminate recombination process<sup>30–33</sup>



Good examples are provided by hydroxyarenes (ROH dyes), such as 1-naphthol, 2-naphthol, and their derivatives, that become strong acids in the first electronically excited state.<sup>11–15,20,21</sup> Light serves here as an ultrafast trigger for PTTS. Excluding their transient nature, ROH photoacids resemble ground-state proton acids. One can characterize their acidic strength by assigning an excited-state equilibrium constant ( $K_a^* = k_d/k_a$ ) to the proton dissociation reaction. In such a treatment, both proton dissociation and recombination steps should be fast compared to the excited-state lifetimes of the protonated (ROH\*) and deprotonated (RO<sup>−\*</sup>) forms of the excited photoacid. Thus, both steps occur reversibly on the excited-state potential surface. Reversibility is manifested even in isolated-pair kinetics, where the geminate proton has a finite probability to recombine with the RO<sup>−\*</sup> anion. Indeed, it was shown, both experimentally<sup>30–32</sup> and theoretically,<sup>34</sup> that geminate recombination slows the apparent ROH\* decay rate. The fingerprint of reversible pair kinetics is the observation of a long time  $t^{-3/2}$  dependence of the ROH\* survival probability.

In PTTS the solvent serves as the base namely, the proton acceptor. Alternately, one may introduce a given concentration of a base, B, into the solution. Weller<sup>12,13</sup> was the first to monitor the kinetics between an excited photoacid (2-naphthol) and anionic bases



Using steady-state fluorescence, he has found a rate constant of  $2.9 \times 10^9 \text{ M}^{-1} \text{ s}^{-1}$  for the reaction between 2-naphthol and acetate in water.<sup>13</sup> Trieff and Sundheim<sup>35</sup> monitored the same reaction in water/glycerol mixtures, finding a decrease in the rate constant with increasing viscosity. (Similar studies of electron-transfer reactions have also been carried out<sup>17b</sup>). Laws

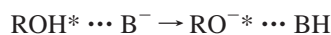
\* Corresponding author: Raymond and Beverly Sackler Faculty of Exact Sciences, School of Chemistry, Tel Aviv University, Tel Aviv 69978, Israel. E-mail: huppert@tulip.tau.ac.il. Fax: 972-3-6407012.

**TABLE 1: Physical Attributes for Water/Glycerol Mixtures and Kinetic Parameters for 2N6S Deprotonation Therein**

vol % glycerol	mol % glycerol	$\epsilon^a$	$R_D^b$ , [Å]	$D_{H^+}^c$ , [ $10^{-5}$ cm $^2$ s $^{-1}$ ]	$k_d^d$ , [10 $^8$ s $^{-1}$ ]	$k_a^e$ , [10 $^8$ s $^{-1}$ ]	$\eta/\eta_w^f$	$\eta/\eta_w^g$	$D^h$ , [10 $^{-5}$ cm $^2$ s $^{-1}$ ]	$b^i$
0	0	78	7.1	9.7	14	8.1	1.00	1.00	0.97	0.0042
10	3.00	74	7.5	7.0	5.7	4.7	1.36	2.27	0.45	0.0085
20	5.82	71	7.8	5.0	4.0	3.0	1.94	2.98	0.26	0.0029
30	9.72	68	8.1	3.0	2.5	2.0	3.08	3.87	0.17	0.0010
40	14.0	65	8.5	2.0	2.0	1.3	4.43	6.21	0.115	0.0056
50	20.2	61	9.1	1.3	1.6	0.8	8.33	11.1	0.067	0.0022
60	26.9	58	9.5	1.0	0.8	0.5	13.6	21.7	0.040	0.017
70	36.9	53	10	0.7	0.2	0.3	40.5	43.1	0.023	0.0095

<sup>a</sup> Static dielectric constant, from ref 48. <sup>b</sup> Debye length, eq 8, for 2N6S in water–glycerol binary mixtures. <sup>c</sup> The proton diffusion coefficient in the presence of 2 M NaClO<sub>4</sub> derived from the computer fit to the experimental PTTS data in Figure 2b. <sup>d</sup> Proton dissociation rate constant measured in water–glycerol binary mixtures, see Figure 2a. <sup>e</sup> Proton dissociation rate constant measured with added 2 M NaClO<sub>4</sub>, see Figure 2b. <sup>f</sup> Solution viscosity (without NaAc) relative to that of neat water ( $\eta_w$ ), taken from ref 49. <sup>g</sup> Solution viscosity relative to neat water ( $\eta_w$ ), after adding 2 M NaAc, from the present work. <sup>h</sup> The mutual diffusion coefficient of 2N6S and acetate derived by fitting the Smoluchowski model in eqs 2–6 to the experimental data in Figure 2b. <sup>i</sup> Relative amplitude of the fluorescence background used in eq 17.

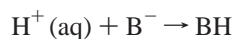
and Brand<sup>36</sup> were the first to monitor it in the time-domain, fitting a biexponential to the decaying fluorescence signal. It was pointed out<sup>37</sup> that Weller’s effective rate constant might be limited by diffusion, so that the “intrinsic” proton-transfer rate parameter which we call  $k_{PT}$  (to differentiate from Weller’s overall rate constant  $k_B$ ) may be somewhat higher  $k_{PT} = 6.5 \times 10^9$  M $^{-1}$  s $^{-1}$ . Probably the 2-naphthol reaction is not severely limited by diffusion because Pines and co-workers,<sup>38</sup> who have applied extremely large base concentrations in order to measure the direct proton transfer within a photoacid–base pair that has preformed already in the ground state,



find (in 8 M acetate) the same rate constant as Weller’s.

For more reactive photoacids they have found considerably larger values for  $k_{PT}$ , which are otherwise masked by diffusion (diffusion rate constant  $k_D$ ). For example, for the reaction between excited 8-hydroxypyrene-1,3,6-trisulfonate (HPTS) and acetate they report  $k_{PT} = 9 \times 10^9$  M $^{-1}$  s $^{-1}$ . Using a femtosecond pump–probe technique, some of us have recently reported a value which is an order of magnitude larger.<sup>39</sup> This shows that the intrinsic bimolecular PT rate constant is both hard to determine and larger than  $k_D$  for exothermic reactions.

Another complication with photoacids such as HPTS is their fast PTTS and recombination rate coefficients,  $k_d$  and  $k_a$ . For small base concentrations (for example, in the 10 mM range) the effective decay rate becomes faster because the base scavenges the solvated proton from solution<sup>33</sup>



before it can recombine with the RO $^{-*}$ . The process speeds up because of the elimination of (geminate) recombination, rather than by the direct acid–base reaction of eq 1. In order for the direct PT reaction to dominate over PTTS, large base concentrations are required. We apply 2 M acetate, as compared with concentrations on the order of 10 mM used by Weller.<sup>12</sup>

The observation that photoacids have intrinsic PT rate constants which are larger than  $k_D$  suggests that one should be able to observe the transient phase of the Smoluchowski dynamics. Weller must have been aware of this possibility, since he has written a theoretical paper<sup>40</sup> on the Smoluchowski theory for fluorescence quenching. Yet his steady-state measurements on the 2-naphthol/acetate system did not reveal nonlinear Stern–Volmer behavior.<sup>12,13</sup> Pines et al.<sup>38</sup> have reported exponential decay for over 3 decades in time for the reaction between HPTS and 1 M of potassium formate in water. The conclusion was

that the transient phase of the Smoluchowski dynamics was unimportant here. This was the situation prevailing prior to our work.

Since we have suspected that the nonexponentiality might occur below the time resolution of the time-correlated single photon counting (TCSPC) technique<sup>5</sup> used, some of us have conducted a femtosecond pump–probe study ( $\sim 150$  fs time resolution) of the HPTS/acetate reaction in aqueous solutions containing 0.5–4 M of sodium acetate (NaAc).<sup>39</sup> Although nonexponential Smoluchowski dynamics were observed, they are convoluted with the ultrafast water dynamics. In addition, the pump–probe signal is a complicated mixture of  $S_1 \rightarrow S_2$  absorption with  $S_1 \rightarrow S_0$  stimulated emission. Spontaneous (TCSPC) fluorescence measurements, though limited in their time resolution, are simpler to interpret and also possess better signal-to-noise ratio.

To allow observation of the early transient phase using spontaneous emission, the relative acid/base diffusion had to be slowed for example, by increasing the solvent viscosity. We have chosen to work in water–glycerol mixtures<sup>35</sup> in which the relative acid–base diffusion coefficient decreases by a factor of 40 with increasing solvent viscosity. The preliminary report<sup>41</sup> of our findings is extended below to a detailed presentation. Using TCSPC, we monitor excited-state proton-transfer from a 2-naphthol derivative to an acetate anion in water–glycerol mixtures of varying compositions. The transient kinetics are compared quantitatively with the Smoluchowski theory, using numerical and approximate solutions for the time-dependent rate coefficient  $k(t)$  and a minimal number of adjustable parameters. Our work demonstrates, for the first time, that fast irreversible chemical reactions can indeed exhibit a pronounced nonexponential phase in quantitative agreement with this classical theory of diffusion-controlled reactions.

## Experimental Methods and Data Analysis

The photoacid under investigation, 2-naphthol-6-sulfonate (2N6S), was dissolved in water–glycerol mixtures as its monosodium salt (TCI, >99% chemically pure). Mixture compositions are given in Table 1. Sodium acetate (NaAc, A. R.) was purchased from Aldrich. 2N6S sample concentrations were between (2 and 5)  $\times 10^{-4}$  M. Deionized water had resistance >10 M $\Omega$ . Glycerol was purchased from Fluka (puris grade). All chemicals were used without further purification. The solution pH was about 7. For the NaAc solutions, the pH was adjusted to around 7 by adding anhydrous acetic acid (Aldrich, A. R.) until the RO $^-$  peak disappeared from the absorption spectrum. Steady-state fluorescence spectra of our samples were

**TABLE 2: Kinetic Parameters for 2N6S/Acetate Reaction in Water for Different NaAc Concentrations, as Obtained from the Data in Figure 4<sup>a</sup>**

$c$ , [M]	$\eta/\eta_w$	$D$ , [ $10^{-5}$ cm <sup>2</sup> s <sup>-1</sup> ]	$a_e$ , [Å]	$e^{-\beta U(a)}$	$k_d$ , [ $10^8$ s <sup>-1</sup> ]	$k_{\text{eff}}$ , [ $10^{10}$ s <sup>-1</sup> ]	$k_D$ , [ $10^9$ M <sup>-1</sup> s <sup>-1</sup> ]	$k_{\infty}$ , [ $10^9$ M <sup>-1</sup> s <sup>-1</sup> ]
0.5	1.12	1.56	5.4	0.45	12.6	0.36	6.3	4.4
1.0	1.32	1.33	5.9	0.53	11.2	0.61	5.9	4.9
2.0	1.72	1.02	6.3	0.61	8.1	1.09	4.9	5.0
3.0	2.12	0.83	6.5	0.66	5.8	1.37	4.1	4.3
4.0	2.69	0.65	6.6	0.69	4.5	1.59	3.2	3.8

<sup>a</sup> From independent experiments, we have obtained the dissociation rate parameter,  $k_d$  (measured in identical NaClO<sub>4</sub> concentrations), and the viscosities relative to neat water ( $\eta_w$ ).  $a_e$  and  $e^{-\beta U(a)}$  are from eqs 11 and 7, respectively. See text for discussion of diffusion coefficients.

recorded on an SLM-AMINCO-Bowman 2 luminescence spectrometer and corrected according to manufacturer specifications. All experiments were performed at room temperature (ca. 22 ± 2 °C).

Time-resolved fluorescence decay was measured using the TCSPC technique. As an excitation source, we used a cw mode-locked Nd:YAG pumped dye laser (Coherent Nd:YAG Antares and a 702 dye laser) providing short pulses (2 ps at full width half-maximum, fwhm) at 300 nm with a high repetition rate (>1 MHz). The TCSPC detection system is based on a Hamamatsu 3809U photomultiplier, Tennelec 864 TAC, Tennelec 454 discriminator, and a personal computer-based multichannel analyzer (nucleus PCA-II). The overall instrument response function (IRF) had a width of about 50 ps (fwhm). Measurements were taken at 350 nm over a 10 nm spectral width. For each water/glycerol mixture we have made three independent measurements: 1. With both 2N6S and NaAc present; 2. with acetate only; and 3. with 2N6S and 2 M NaClO<sub>4</sub> replacing the NaAc. Measurements with acetate only gave small fluorescence background from the salt solution, which was subtracted from the signal of samples containing both photoacid and acetate to produce the observed intensity signal  $I_{\text{obs}}(t)$ . The sample with the NaClO<sub>4</sub> salt was used to determine  $k_d$ , under identical ionic strength to that in the actual measurement.

**Viscosity Measurements.** To correctly fit our experimental data we need an estimate for the relative 2N6S/Ac<sup>-</sup> diffusion coefficient that, by Stokes law, is expected to scale with solvent viscosity.<sup>42</sup> Therefore, we conducted viscosity ( $\eta$ ) measurements of water-glycerol mixtures containing 2 M sodium acetate using an Ostwald viscometer. In this apparatus, the viscosity is measured by noting the time ( $t$ ) required for the liquid to drain between two marks on the capillary tube. It is compared to the time ( $t^0$ ) for a known standard sample using the relation  $\eta^0/\eta = t^0/t$ , where  $\eta$  and  $\eta^0$  are the viscosities of the unknown sample and the standard, respectively. Three viscosity measurements were averaged for each solution at room temperature, 22 °C (295 K). Table 1 shows the values of the measured relative viscosities of our samples.

In addition, we need to take into account the slower diffusion due to the added NaAc salt. Using similar methods, we have measured (see also ref 39) the viscosity (relative to water) of aqueous solutions containing 0.5–4 M of NaAc (Table 2).

### The Smoluchowski Model

According to the Smoluchowski model, the survival probability of a single (static) donor (here, ROH\*) due to its irreversible reaction with a concentration  $c = [\text{B}^-]$  of acceptors is given by<sup>22,25,27</sup>

$$S(t) = \exp[-c \int_0^t k(t') dt'] \quad (2)$$

where  $k(t)$  is the time-dependent rate coefficient (or, reactive

flux at the contact distance  $a$ ) for the donor–acceptor pair

$$k(t) = k_{\text{PT}} p(a, t) \quad (3)$$

whose proton-transfer rate constant is  $k_{\text{PT}}$ . The pair (ROH\*/B<sup>-</sup>) density distribution  $p(r, t)$  is governed by a Smoluchowski equation [diffusion in a potential  $U(r)$ ] in three dimensions<sup>1</sup>

$$\partial p(r, t) / \partial t = D r^{-2} \frac{\partial}{\partial r} r^2 e^{-\beta U(r)} \frac{\partial}{\partial r} e^{\beta U(r)} p(r, t) \quad (4)$$

where  $D$  is the relative diffusion coefficient of the pair,  $U(r)$  their interaction potential, and  $\beta = 1/k_B T$  and  $k_B T$  is the thermal energy. To calculate  $k(t)$ , one imposes an initial equilibrium distribution

$$p(r, 0) = \exp[-\beta U(r)] \quad (5)$$

and a “radiation” boundary condition at the contact distance ( $r = a$ ), depicting irreversible recombination occurring upon the binary collision<sup>23</sup>

$$4\pi D a^2 e^{-\beta U(a)} \frac{\partial}{\partial r} e^{\beta U(r)} p(r, t) |_{r=a} = k_{\text{PT}} p(a, t) \quad (6)$$

One of the goals of our study is to determine the intrinsic bimolecular rate coefficient  $k_{\text{PT}}$ .

The interaction potential  $U(r)$  was taken as the Debye–Hückel (DH) screened Coulomb potential,<sup>42</sup>

$$\beta U(r) = (R_D/r) e^{-\kappa(r-a)} / (1 + \kappa a) \quad (7)$$

for the electrostatic repulsion within the negatively charged 2N6S/Ac<sup>-</sup> pair, with screening due to the NaAc salt. Both the Debye length  $R_D$  and the inverse of the DH screening length  $\kappa$  may be calculated from the static dielectric constant of the solutions  $\epsilon$  (see Table 1) according to

$$\kappa^2 = 8\pi\beta e^2 c / \epsilon, \quad R_D = \beta e^2 / \epsilon \quad (8)$$

where  $e$  is the electronic charge. Thus  $R_D = 7.1$  Å for neat water, increasing with the addition of the low-dielectric cosolvent. These parameters for the various water-glycerol mixtures are collected in Table 1.

Although the DH theory is inaccurate at high salt concentrations, for a 2 M salt solution  $1/\kappa \approx 2$  Å is so small that the effect of the potential on the results is only marginal. We have solved eq 4 numerically, using a user-friendly Windows application for Spherically-Symmetric Diffusion Problems (SSDP, version 2.61)<sup>43</sup> to yield  $k(t)$  of eq 3. Only one physical parameter was varied from solvent to solvent, the diffusion coefficient  $D$ , and it was compared with our independent viscosity measurements.

For  $U(r) \equiv 0$  it is possible to solve the above equations analytically for  $k(t)$ .<sup>26</sup> This is no longer true when  $U(r) \neq 0$ . In this case, Szabo<sup>27</sup> has found an approximate expression for the

time dependent rate constant:

$$k(t) = \frac{4\pi Da_e k_{PT} e^{-\beta U(a)}}{k_{PT} e^{-\beta U(a)} + 4\pi Da_e} \times \left\{ 1 + \frac{k_{PT} e^{-\beta U(a)}}{4\pi Da_e} e^{\gamma^2 Dt} \operatorname{erfc}[(\gamma^2 Dt)^{1/2}] \right\} \quad (9)$$

where  $\gamma$  is given by

$$\gamma = a_e^{-1} \left( 1 + \frac{k_{PT} e^{-\beta U(a)}}{4\pi Da_e} \right) \quad (10)$$

$\operatorname{erfc}$  is the complementary error function and  $a_e$  is an effective radius defined by

$$a_e^{-1} = \int_a^\infty e^{\beta U(r)} r^{-2} dr \quad (11)$$

Equation 9 is exact when the potential is zero, i.e.,  $U = 0$  and  $a_e = a$ . When a potential is introduced, it behaves correctly at both  $t = 0$  and  $t = \infty$  limits

$$k(0) = k_{PT} e^{-\beta U(a)}, \quad k(\infty) = [k(0)^{-1} + k_D^{-1}]^{-1} \quad (12)$$

where  $k_D = 4\pi Da_e$  is the diffusion-control rate constant. The nonexponentiality in  $S(t)$  is a result of a nonconstant  $k(t)$ , as depicted by the ratio  $k(0)/k(\infty) = 1 + k(0)/k_D = \gamma a_e$ . It depends on the factor  $\gamma a_e$ , but not on  $\gamma$  alone. In contrast, the transient behavior is determined by the value of  $\gamma$  appearing in the  $\operatorname{erfc}$  term. With  $\gamma$  from eq 10, eq 9 exhibits the correct time behavior also at asymptotically large times,<sup>26</sup>

$$k(t) \rightarrow k(\infty) \left[ 1 + \left( \frac{a_e k(0)}{k(0) + k_D} \right) \frac{1}{\sqrt{\pi Dt}} \right] \quad (13)$$

but not for intermediate time spans. For the latter case, Szabo<sup>27</sup> derived an alternative expression for  $k(t)$  that has the same functional form as eq 9 but with  $\gamma$  replaced by  $\gamma'$ , where

$$\gamma' = \gamma a_e^2 e^{\beta U(a)} / a^2 \quad (14)$$

This result has been previously obtained by Weller<sup>40</sup> and by Flannery.<sup>44</sup> When this  $\gamma'$  correction is used in eq 9, the asymptotic behavior of eq 13 no longer holds.

From the time dependent rate constant,  $k(t)$ , one can calculate the survival probability of an ROH\* molecule surrounded by an equilibrium distribution of ions, according to eq 2. To account for PTTS, which occurs in parallel (with a time constant  $\tau_d \equiv 1/k_d$ ), and supposedly independently from the reaction in eq 1, we write

$$S'(t) = \exp[-t/\tau_d - c \int_0^t k(t') dt'] \quad (15)$$

This quantity, with an independently measured  $\tau_d$ , is used to compare with the corrected experimental signal  $I_{\text{corr}}(t)$ , see below.

## Results and Discussion

**Steady-State Fluorescence.** The steady-state emission of 2N6S consists of two structureless broad bands, the maxima of which are at 355 and 430 nm (Figure 1). Their relative intensity depends on the solution pH (not shown). The peak at 355 nm, which increases with proton concentration, is assigned to ROH\*,

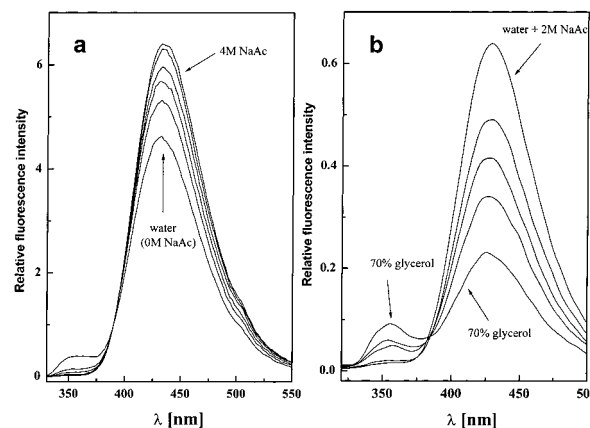


**Figure 1.** Steady-state fluorescence spectra of 2N6S (a) in water containing 0, 0.5, 1, 2, 3 and 4 M of NaAc; (b) in mixtures of water + 2 M NaAc with 10, 30, 50, and 70% glycerol by volume. Excitation wavelength: 300 nm.

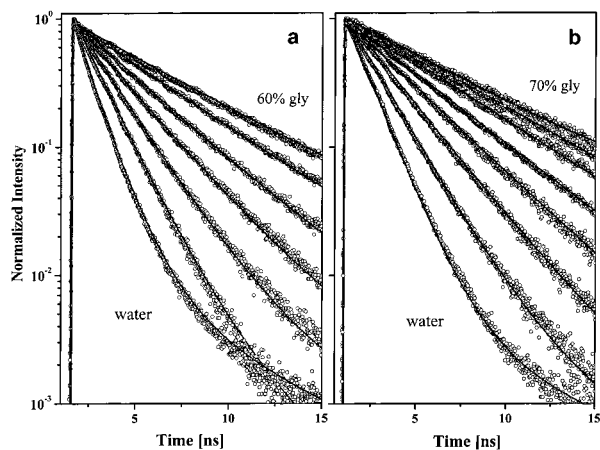
whereas the decreasing peak (at 430 nm) is that of the RO<sup>-\*</sup> form. In our time-resolved measurements we follow the ROH\* decay at 350 nm, slightly to the blue of the ROH\* band in order to avoid overlap with the RO<sup>-\*</sup> band.

Figure 1 shows the steady-state fluorescence as a function of (a) acetate-base concentration in water and (b) the solution glycerol content (for 2 M acetate). The isoemissive point seen in both cases is another indication for the existence of two emitting states (ROH\* acid, RO<sup>-\*</sup> base). Figure 1a shows that as the concentration of the acetate base increases, the ROH\* emission decreases, whereas the RO<sup>-\*</sup> emission increases due to the reaction in eq 1. Incidentally, this also shows that proton scavenging by acetate does not quench the fluorescence, leaving behind an excited anion. Figure 1b shows that as the volume fraction of glycerol increases, the RO<sup>-\*</sup> band decreases and that of ROH\* increases in intensity, indicating a slower bimolecular proton-transfer reaction 1 with increasing solvent viscosity. In both cases, the peak frequencies do not appear to depend on the solution composition. Hence (unlike the situation considered by Pines et al.<sup>38</sup>) neither the increasing acetate concentration (up to 4 M) nor the lower dielectric constant of the glycerol-containing mixtures induce any ion-pair formation.

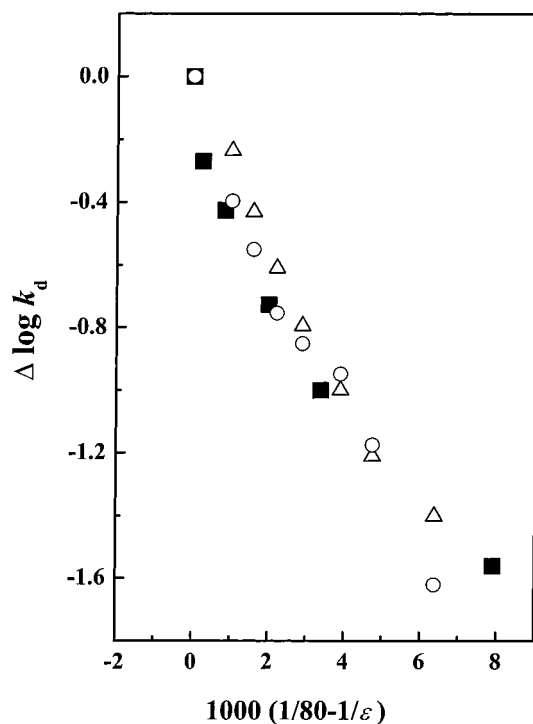
**Proton Transfer to Solvent.** First we have investigated the transient PTTS kinetics in the absence of the Ac<sup>-</sup> base. Figure 2a shows the ROH\* emission (circles) in binary mixtures of water-glycerol containing 0–60 vol % (0–0.3 mole fraction) of glycerol. As can be seen, the larger the glycerol content the slower the PTTS rate. The lines are a fit to the transient solution of a Smoluchowski equation depicting reversible geminate recombination. This approach is described in detail elsewhere.<sup>30–32</sup> The PTTS rate constant  $k_d$  is given in Table 1 together with the corresponding values for the proton diffusion coefficient,  $D_{H^+}$  and the Debye radius  $R_D$ . Figure 2b shows similar data in the presence of 2 M of an inert electrolyte, NaClO<sub>4</sub>. This reduces the values of  $k_d$ , as seen in Table 1. We have also measured  $k_d$  in water for different electrolyte (NaClO<sub>4</sub>) concentrations (not shown), and these data are collected in Table 2.  $k_d$  decreases in the presence of the added electrolyte (by about 20% at 2 M). Lee<sup>45</sup> has found a similar reduction in the presence of 2 M of LiCl, attributing it to the loss of “free” water, which becomes coordinated to either cations or anions and is thus unavailable for solvating the proton.

Figure 3 shows the relative rate constant,  $k_d(\text{mix})/k_d(\text{water})$  as a function of  $1/\epsilon$  ( $\epsilon$  is the dielectric constant of the solvent mixture) for 2N6S (open symbols) along with similar data





**Figure 2.** Time-resolved emission of 2N6S in water-glycerol mixtures. Bottom up: glycerol volume content increases from 0% in 10% increments. (Open circles) experimental data, and (full line) fit to the solution of the Smoluchowski equation for a geminate pair with reversible boundary conditions, as described in ref 30. (a) Without added electrolyte and (b) with 2 M sodium perchlorate.



**Figure 3.** Semilog plot of the PTTS rate constants as a function of  $1/\epsilon$ . (Open symbols) 2N6S in glycerol/water mixtures (Table 1): (circles) w/out salt and (triangles) with 2 M NaClO<sub>4</sub>. (Solid squares) HPTS in methanol/water mixtures (from ref 46).

(squares, ref 46) for HPTS in water–methanol mixtures. Even though 2N6S and HPTS have different charges and molecular sizes, their relative dissociation parameters fall approximately on the same curve.

**Direct Acid–Base Reaction in Water.** We now turn to the main goal of our work, which is the study of direct acid–base reactivity in the excited-state, eq 1. To show that this mechanism indeed occurs, we have first investigated the dependence of the observed kinetics on the concentration of the (acetate) base (0.5–4 M) in neat water (no glycerol added). The results in Figure 4 exhibit fast decay of the fluorescence signal—much faster than the decay due to the PTTS process depicted in Figure 2. The decay becomes even faster with increasing  $c$ . This gives

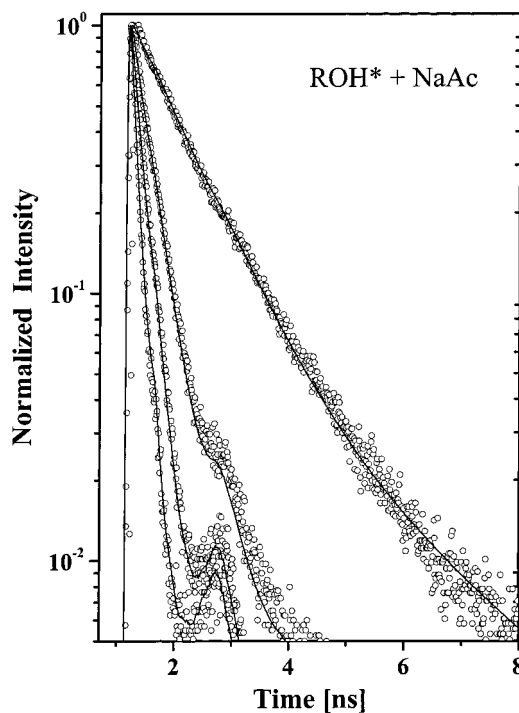


**Figure 4.** Time-resolved emission of 2N6S in neat water with various NaAc concentrations: (top to bottom) 0.5, 1, 2, and 4 M (circles), with (IRF convoluted) single-exponential fits (line). The values of  $k_{\text{eff}}$  extracted from these fits are collected in Table 2.

clear indication that a bimolecular acid–base reaction dominates the kinetics (and not, for example, the scavenging of the solvated protons<sup>33</sup>).

As observed by Pines et al.<sup>38</sup> for HPTS, the decay of 2N6S is also single exponential over about 99% of the intensity scale. We have to exclude the last 1% from the analysis because (i) the decay becomes so fast that a small (1%) secondary peak in the IRF interferes and produces a bump in the fluorescence signal and (ii) because of interference from fluorescing impurities. On the basis of the HPTS pump–probe measurements,<sup>39</sup> we assume that we could be missing fast components that are beyond the TCSPC resolution. These may include the initial nonexponential decay of the Smoluchowski kinetics, as well as dynamic solvation effects. We therefore conclude that in water we are monitoring the long-time limit of the Smoluchowski model, with the rate coefficient  $k(\infty)$ , see eq 12.

Since this reaction occurs in parallel to the slower unimolecular dissociation (rate constant  $k_d$ ) and excited-state decay (rate constant  $k_0$ ), we expect an effective rate constant

$$k_{\text{eff}} = ck(\infty) + k_d + k_0 \quad (16)$$

We obtain  $k_{\text{eff}}$  by fitting the data in Figure 4 to  $\exp(-k_{\text{eff}}t)$ , convoluted with the (measured) IRF. It is plotted as a function of  $c$  in Figure 5a. We have chosen the log–log scale so that we can display also  $k_d$  on the same scale. As already noted, proton-transfer rate constants decrease with increasing salt concentration.<sup>45,47</sup> The fact that  $k_{\text{eff}}$  (in contrast to  $k_d$ ) increases almost linearly with  $c$ , is in line with the behavior expected from bimolecular kinetics. Up to 4 M NaAc, we find no indication for effective unimolecular kinetics within preformed acid–base pairs.<sup>38</sup> We believe the reason that  $k_{\text{eff}}$  is slightly sublinear at the high concentrations (3–4 M) is the decrease in  $k(\infty)$  and  $k_d$  with added electrolyte.

Using the measured values of  $k_0$  and  $k_d$ , we can now obtain (eq 16) the steady-state acid–base reaction rate coefficient,  $k(\infty)$ .

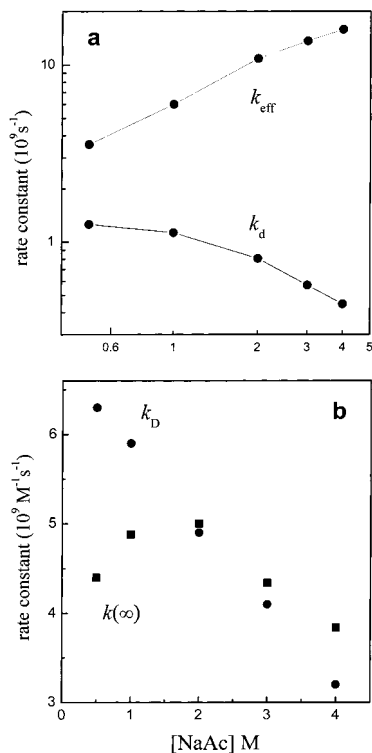


**Figure 5.** Concentration dependence of the rate constants of Table 2. (a) The unimolecular and (b) the bimolecular rate constants.

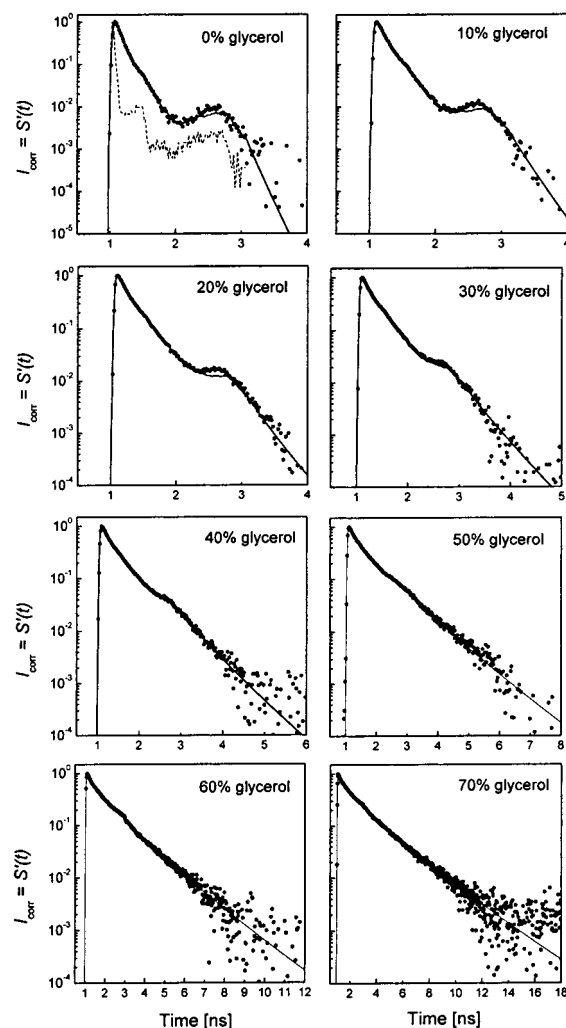
Weller<sup>13</sup> has determined the excited-state lifetime,  $\tau_0 = 1/k_0$ , for 2N6S as 6.5 ns for the ROH\* form and 13.5 ns for RO<sup>-\*</sup>. These times are slow relative to the other processes involved. In our analysis we use an average value of 10 ns. The  $k_d$  values are collected in Table 2.

Figure 5b compares the concentration dependence of  $k(\infty)$  with that of the diffusion-control rate constant  $k_D = 4\pi D a_c$  (our independent determination of  $D$  is described below). In line with the Onsager theory,<sup>42</sup>  $k_D$  decreases with increasing  $c$ . In contrast,  $k(0)$  in eq 12 increases with  $c$  due to the enhanced screening which facilitates the approach of the two negative ions. Thus,  $k(\infty)$  is dominated at low concentrations by  $k(0)$  and at high concentrations by  $k_D$ . As Figure 5b shows,  $k(\infty)$  first increases with  $c$  but above 2 M it becomes diffusion limited. Hence it is only below 2 M that we may use eq 12 to obtain  $k(0)$  and, from it, the intrinsic proton-transfer rate parameter  $k_{\text{PT}}$ . In this manner we estimate that  $k_{\text{PT}} = (3-5) \times 10^{10} \text{ M}^{-1} \text{ s}^{-1}$ , about an order of magnitude larger than the rate constant for the reaction of 2-naphthol with acetate.<sup>12,13,37</sup> Better estimates may require femtosecond time resolution and may suffer from the interference of dynamic solvation processes.<sup>39</sup>

#### Direct Acid–Base Reaction in Glycerol–Water Mixtures.

To enhance the initial nonexponential behavior predicted by the Smoluchowski theory, we have decreased the diffusion coefficient by adding a very viscous cosolvent namely, glycerol. By increasing the glycerol content up to 0.4 mole fraction,  $D$  decreased by a factor of 40 (see Table 1). The slower decay also resulted in less interference from the secondary peak in the IRF. To unravel the nonexponential Smoluchowski dynamics requires careful treatment of the data over nearly 4 orders of intensity. The observed fluorescence intensity of the ROH\* form of 2N6S,  $I_{\text{obs}}(t)$ , was corrected for the excited-state lifetime,  $\tau_0 = 1/k_0$ , and a constant background,  $b$ , according to

$$I_{\text{corr}}(t) = [I_{\text{obs}}(t) \exp(t/\tau_0) - b]/N \quad (17)$$



**Figure 6.** Time-resolved emission of 2N6S in water–glycerol mixtures in the presence of 2 M NaAc (dots) along with a fit to the numerical solution of the Smoluchowski model in eqs 2–6 (full line). The relative 2N6S/Ac<sup>-</sup> diffusion coefficients,  $D$ , were adjusted at each composition (Table 1), whereas the intrinsic rate-transfer constant was kept constant,  $k_{\text{PT}} = 9.4 \times 10^9 \text{ M}^{-1} \text{ s}^{-1}$ . The IRF is shown in the upper-left panel (dashed line).

$\tau_0 = 10$  ns, and it was assumed constant for all glycerol compositions. The background is attributed to a small degree of dimerization or degradation of the photoacid.  $I_{\text{corr}}(t)$  was subsequently compared with the theoretical survival probability from the Smoluchowski model,  $S'(t)$  of eq 15, after convoluting it with the (independently measured) IRF. The normalization factor,  $N$  in eq 17, was chosen so that the amplitude of  $I_{\text{corr}}(t)$  agrees with that of the (convoluted)  $S'(t)$ . The PTTS rate coefficient,  $k_d$ , was measured separately (Figure 2) and reported in Table 1. The time dependent rate coefficient  $k(t)$  that goes into the evaluation of  $S(t)$  was calculated from a numerical solution of the Smoluchowski eq 4 with initial and boundary conditions from eqs 5 and 6, using the SSDP software<sup>43</sup> with the parameters of Table 1. The same software also performed the required numeric integration.

The main effort in this study, to measure the 2N6S kinetics at a constant base concentration while the mutual diffusion constant changes by a large factor, is summarized in Figure 6. It shows the ROH\* emission (circles),  $I_{\text{corr}}(t)$ , measured in water–glycerol mixtures containing 2N6S with 2 M of NaAc. The dashed line in the 0% glycerol panel shows the IRF, with which  $S'(t)$  of eq 15 was convoluted (full lines). The larger the

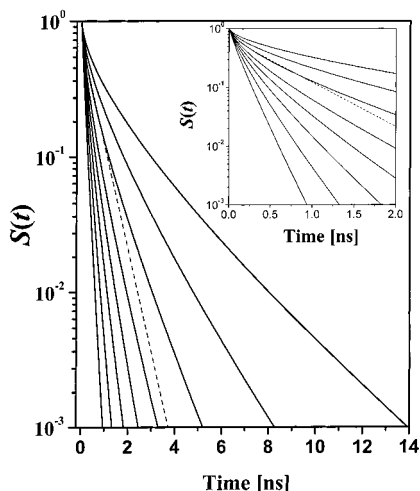


**Figure 7.** Calculated (eq 2) survival probabilities of ROH\* in the presence of 2 M NaAc for various solvent compositions (bottom upward): 0, 10, 20, 30, 40, 50, 60, and 70% (vol) of glycerol (semilog scale). Obtained from the fits shown in Figure 6. The dashed line is a biexponential fit to the short time behavior in 50% (vol) glycerol. The inset shows the initial decay of  $S(t)$ .

glycerol mole fraction, the stronger the deviation from exponential decay.

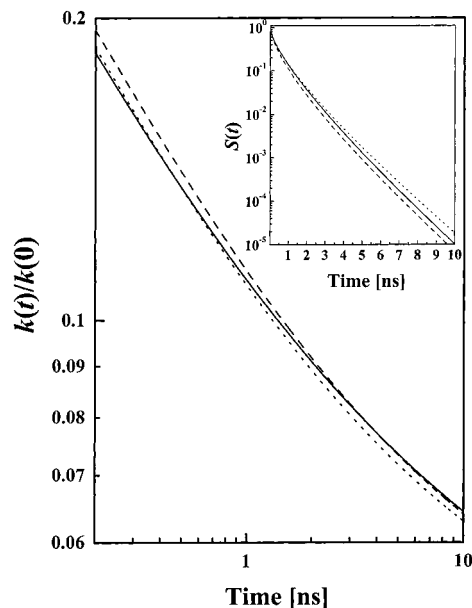
The effect may be better appreciated in a plot comparing  $S(t)$ , eq 2, for the various compositions (Figure 7). This presentation, in effect, deconvolutes the data from the IRF, and eliminates the herein irrelevant contribution to the fluorescence decay from the PTTS process and the finite excited-state lifetime. The dashed line shows a biexponential fit for one of the solution compositions, such as may be expected from a conventional chemical kinetic treatment.<sup>31</sup> As shown in the inset, this can only fit the first 1 ns of the decay in  $S(t)$ . Thus, for the reaction under investigation, the Smoluchowski model appears indispensable for reproducing the correct time behavior. In fact,  $k(t)$  varies so rapidly with time, that the initial exponential decay, with the (almost) composition independent  $k(0)$ , occurs on such short time scales that are beyond the resolution of our experiment.

Figure 8 shows  $k(t)$ , calculated by solving numerically eqs 3–7 using SSDP version 2.61 (line),<sup>43</sup> as compared with the analytical approximation<sup>27</sup> in eq 9 using either  $\gamma$  (eq 10, dashed line) or  $\gamma'$  (eq 14, dotted line). As can be seen, in the first case the approximate  $k(t)$  does indeed approach the correct asymptotic behavior (eq 13), whereas the use of  $\gamma'$  gives an improved description of the short time behavior. (Interestingly, this short time behavior is approximately a power law). These approximate  $k(t)$  overestimate (underestimate) the exact solution, and as a result the approximate  $S(t)$  underestimate (overestimate) the exact survival probability (inset). Consequently, one may improve eq 9 empirically by switching between  $\gamma'$  and  $\gamma$  according to

$$\gamma'' = \gamma' + (\gamma - \gamma')(1 - e^{-t/\theta}) \quad (18)$$

Here  $\theta$  is an adjustable parameter changing gradually from 500 ps (for neat water) to about 4 ns at 0.4 mole fraction of glycerol. The approximation involving  $\gamma''$  in place of  $\gamma$  in eq 9 is indistinguishable from the exact numerical solution.

**The Fitting Parameters.** In the present analysis, most of the model parameters are known from published literature values. Literature values for the dielectric constants  $\epsilon$ ,<sup>48</sup> and the viscosities  $\eta$ ,<sup>49</sup> of these mixtures are given in Table 1. Following Weller,<sup>12,13</sup> we take the contact radius  $a$  as 7 Å. This



**Figure 8.** Comparison of  $k(t)$  calculated numerically (line) with the prediction of eq 9 using  $\gamma$  (eq 10, dashed line) and  $\gamma'$  (eq 14, dotted line) for 20 mol % of glycerol.<sup>27</sup> Note the log–log scale. Inset:  $S(t)$ , on a semilog scale, calculated by integrating these three  $k(t)$  functions according to eq 2.

leaves us with only two parameters that were adjusted to fit the data:  $k_{PT}$  and  $D$ .

The kinetics at the different glycerol compositions could be fit with the same intrinsic proton-transfer rate constant,  $k_{PT} = 9.4 \times 10^9 \text{ M}^{-1} \text{ s}^{-1}$ . This value is smaller than what we estimated in water, around  $4 \times 10^{10} \text{ M}^{-1} \text{ s}^{-1}$ . As seen in Figure 5b, for  $c \geq 2 \text{ M}$  the reaction in neat water is diffusion-controlled, and thus insensitive to the precise value of  $k_{PT}$ . Therefore, the lower PT rate constant we find in the glycerol mixtures at 2 M acetate must, to an extent, reflect the effect of the added glycerol. It appears that further addition of glycerol (beyond, for example, the first 10 or 20 vol %) does not alter  $k_{PT}$  much. This might indicate that glycerol molecules do not intervene between the proton-donating acid and the proton-accepting base at the time of transfer, so that the structure of the contact pair is independent of solvent composition. Thus, proton-transfer might be mediated by a water molecule, but not by glycerol.

The initial rate constant is  $k(0) = k_{PT}e^{-\beta U(a)}$ , see eq 12. In our case  $U(a)$  results from the Coulomb repulsion between the negatively charged acetate and 2N6S ions.  $U(a)$  is determined by the dielectric constant and the ionic screening. The dielectric constant of water-glycerol mixtures varies with composition, but the overall change is not large (from 78 in neat water to 53 at the highest glycerol content), since neat glycerol also has a high dielectric constant. The screening effect depends strongly on the acetate concentration (eqs 7–8). At 2 M concentration, it reduces the Coulombic repulsion quite dramatically. As a result, given that  $k_{PT}$  is solvent independent,  $k_{PT}e^{-\beta U(a)}$  varies by only a factor of  $\sim 1.5$ .

We estimate that the error in the determination of the initial rate constant,  $k(0) = k_{PT}e^{-\beta U(a)}$ , is about 20%. The error arises from two main contributions: the limited time resolution of the experimental system (fwhm  $\sim 50$  ps), which limits the determination of fast kinetic components, and the solvation dynamics of the reactants that contribute an additional fast component to the luminescence signal at early times overlapping with the actual decay of the ROH\* population.

The marked nonexponentiality, as quantitated by the ratio,  $k(0)/k(\infty) = 1 + k(0)/k_D$ , must therefore be due predominantly

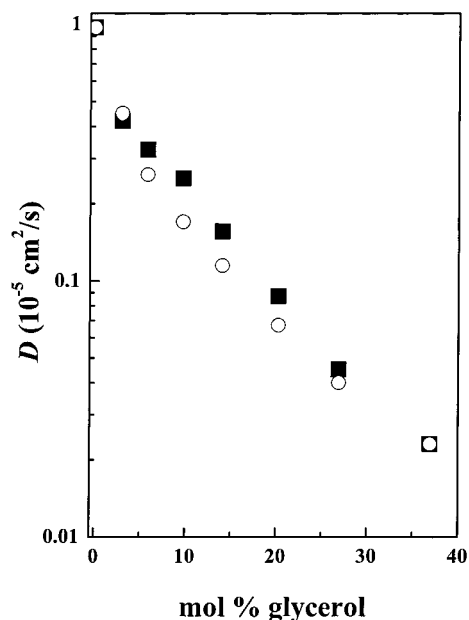


**Figure 9.** Relative acid (2N6S) to base (acetate) diffusion coefficient in water-glycerol mixtures containing 2 M sodium acetate. Circles are from the dynamic fits to the time-resolved data of Figure 6. Squares are the viscosity-scaled water data ( $D_w = 1 \times 10^{-5} \text{ cm}^2 \text{ s}^{-1}$  in 2 M NaAc, see text), according to  $D = \eta_w D_w / \eta$ , using viscosity data (Table 1).

to variations in the diffusion-controlled rate constant  $k_D$ . Indeed, the ratio  $k_{PT} e^{-\beta U(a)} / k_D$ , which in neat water is about 1, increases to 44 in 0.4 mol fraction of glycerol. Because  $k_D = 4\pi D a_e$ , and  $a_e$  depends on the potential (eq 11) which varies only weakly due to screening, the main effect arises (as anticipated) from solvent variations in the diffusion coefficient  $D$ .

The diffusion coefficient can be estimated as follows. For both acetate and 2-naphthol in water, Weller<sup>13</sup> suggested diffusion coefficients of  $1.1 \times 10^{-5} \text{ cm}^2 \text{ s}^{-1}$ . According to a more recent compilation,<sup>50</sup> the values for naphthol derivatives fall in the range  $0.55\text{--}0.65 \times 10^{-5} \text{ cm}^2 \text{ s}^{-1}$ . Taking the upper limit, we estimate that the mutual diffusion constant,  $D = D_{\text{ROH}} + D_{\text{Ac}^-}$ , in water is  $D = 1.75 \times 10^{-5} \text{ cm}^2 \text{ s}^{-1}$ . From our viscosity measurements (assuming Stokes' law<sup>42</sup>), we can estimate  $D$  in water containing various concentrations of NaAc (Table 2). This procedure might be inappropriate for extrapolating to concentrations as high as 4 M (see discrepancy between  $k_D$  and  $k(\infty)$  in Figure 5b), but hopefully for 2 M NaAc it is still reasonable. Here  $D$  diminishes by a factor of about 1.7 as compared to water. As glycerol is added,  $D$  should further diminish in inverse proportion to the relative glycerol viscosity reported in Table 1.

It is interesting to compare the values obtained for  $D$  from our kinetic measurements with the above estimate using our viscosity data. As shown in Figure 9, the two methods for estimating  $D$  agree quite nicely.  $D$  decreases by a factor of over 40 when going from 0 to 70 vol % glycerol, and this is the main effect to which the enhanced nonexponentiality is attributed. Since it was the only physical parameter adjusted for each solvent composition, the agreement with our viscosity measurements is reassuring, lending further support to the Smoluchowski theory.

## Summary

The Smoluchowski approximation is one of the oldest, and perhaps the most well-known results in the kinetics of irreversible, diffusion-influenced reactions.<sup>1</sup> Taking advantage of the

fact that the process ends upon the first donor-acceptor collision, it decouples the many-body effect in bimolecular reactivity into pair kinetics. Since it was first published,<sup>22</sup> more than 50 years have elapsed before it could be seriously tested, predominantly for fluorescence quenching.<sup>4,6</sup> Yet, the results were never really clear-cut.<sup>8</sup> This has left chemists with the impression, that probably the transient phase is not that crucial for chemical kinetics, and thus it suffices to consider exponential kinetics with a time-independent rate constant,  $k_D$ . In proton-transfer reactions, this was indeed the customary approach since Eigen's early work<sup>14</sup> and until recent days.<sup>38</sup>

In the present endeavor, we have moved away from acid-base reactions in pure water to higher viscosity solvents (glycerol-water mixtures). This results in a large decrease of the mutual acid-base diffusion coefficient, accompanied by only a modest decrease in the proton-transfer rate constant. The large factor between the initial activated-rate parameter for proton-transfer and the long-time diffusion-controlled one, lead to marked nonexponential kinetics, which follow the Smoluchowski prediction. The observation of strong nonexponential acid-base kinetics allows us to determine the intrinsic proton-transfer rate parameter  $k_{PT}$ , which exceeds the diffusion control limit.

In water, our time resolution only allows us to observe what appears to be the long-time exponential behavior. From it we estimate that  $k_{PT}$  exceeds  $10^{10} \text{ M}^{-1} \text{ s}^{-1}$  (by a factor 2–5). Femtosecond measurements are required for a more precise determination, though they are going to be sensitive to ultrafast water dynamics that occur simultaneously on these time scales.

**Acknowledgment.** Our work was supported by grants from the Israel Science Foundation (127/99) and the James-Franck German-Israel program in laser-matter interaction. The Fritz Haber Research Center is supported by the Minerva Gesellschaft für die Forschung, mbH, München, FRG.

## Note Added after ASAP Posting

This article was released ASAP on 7/11/2001 with minor errors in Tables 1 and 2. The correct version was posted on 7/16/2001.

## References and Notes

- (1) Rice, S. A. In: *Comprehensive Chemical Kinetics*; Bamford, C. H., Tipper, C. F. H., Compton, R. G., Eds.; Elsevier: Amsterdam, 1985; Vol. 25.
- (2) Sze, S. M. *Physics of Semiconductor Devices*, 2nd ed.; Wiley-Interscience: New York, 1981.
- (3) Birks, J. B. *Photophysics of Aromatic Molecules*; Wiley-Interscience: London, 1970.
- (4) Nemzek, T. L.; Ware, W. R. *J. Chem. Phys.* **1975**, *62*, 477.
- (5) Schulman, E. F. *Fluorescence and Phosphorescence Spectroscopy*; Pergamon Press: New York, 1977.
- (6) Eads, D. D.; Dismar, B. G.; Fleming, G. R. *J. Chem. Phys.* **1990**, *93*, 1136.
- (7) Lakowicz, J. R. In *Topics in Fluorescence Spectroscopy*; Lakowicz, J. R., Ed.; Plenum: New York, 1994; Vol. 4.
- (8) Sikorski, M.; Krystkowiak, E.; Steer, R. P. *J. Photochem. Photobiol. A* **1998**, *117*, 1.
- (9) Berberan-Santos, M. N.; Martinho, J. M. G. *J. Chem. Phys.* **1991**, *95*, 1817.
- (10) Martinho, J. M. G.; Farinha, J. P.; Berberan-Santos, M. N.; Duhamel, J. Winnik, M. A. *J. Chem. Phys.* **1992**, *96*, 8143.
- (11) Förster, T. *Z. Elektrochem.* **1950**, *54*, 531.
- (12) Weller, A. *Z. Elektrochem.* **1954**, *58*, 849.
- (13) Weller, A. *Z. Phys. Chem. N. F.* **1958**, *17*, 224.
- (14) Eigen, M. *Angew. Chem., Int. Ed. Engl.* **1964**, *3*, 1.
- (15) Ireland, J. F.; Wyatt, P. A. H. *Adv. Phys. Org. Chem.* **1976**, *12*, 131.
- (16) Fuos, R. M.; Kraus, C. A. *J. Am. Chem. Soc.* **1933**, *55*, 1019.



- (17) (a) Kuznetsov, A. M.; Ulstrup, J. *Electron Transfer in Chemistry and Biology*; Wiley-Interscience: Chichester, 1999. (b) Angulo, G.; Grampp, G.; Landgraf, S. *J. Inf. Rec.* **2000**, 25, 381.
- (18) Gutman, M.; Nachliel, E.; Kiryati, S. *Biophys. J.* **1992**, 63, 281.
- (19) Holzwarth, A. R. *Methods Enzymol.* **1995**, 246, 334.
- (20) Weller, A. *Prog. React. Kinet.* **1961**, 1, 187.
- (21) Arnaut, L. G.; Formosinho, S. J. *J. Photochem. Photobiol. A* **1993**, 75, 1.
- (22) Von Smoluchowski, M. *Z. Phys. Chem.* **1917**, 92, 129.
- (23) Collins, F. C.; Kimball, G. E. *J. Coll. Sci.* **1949**, 4, 425.
- (24) Noyes, R. M. *Prog. React. Kinet.* **1961**, 1, 129.
- (25) Tachiya, M. *Radiat. Phys. Chem.* **1983**, 21, 167.
- (26) Gösele, U. M. *Prog. React. Kinet.* **1984**, 13, 63.
- (27) Szabo, A. *J. Phys. Chem.* **1989**, 93, 6929.
- (28) Blumen, A.; Zumofen, G.; Klafter, J. *Phys. Rev.* **1984**, B30, 5379; *J. Phys. (Paris)* **1985**, 46, C7–3.
- (29) Szabo, A.; Zwanzig, R.; Agmon, N. *Phys. Rev. Lett.* **1988**, 61, 2496.
- (30) Pines, E.; Huppert, D.; Agmon, N. *J. Chem. Phys.* **1988**, 88, 5620.
- (31) Agmon, N.; Pines, E.; Huppert, D. *J. Chem. Phys.* **1988**, 88, 5631.
- (32) Huppert, D.; Pines, E.; Agmon, N. *J. Opt. Soc. Am.* **1990**, 7, 1545.
- (33) Goldberg, S. Y.; Pines, E.; Huppert, D. *Chem. Phys. Lett.* **1992**, 192, 77.
- (34) Agmon, N.; Szabo, A. *J. Chem. Phys.* **1990**, 92, 5270.
- (35) Trieff, N. M.; Sundheim, B. R. *J. Phys. Chem.* **1965**, 69, 2044.
- (36) Laws, W. R.; Brand, L. *J. Phys. Chem.* **1979**, 83, 795.
- (37) Lawrence, M.; Marzocco, C. J.; Morton, C.; Schwab, C.; Halpern, A. M. *J. Phys. Chem.* **1991**, 95, 10294.
- (38) Pines, E.; Magnes, B.-Z.; Lang, M. J.; Fleming, G. R. *Chem. Phys. Lett.* **1997**, 281, 413.
- (39) Genosar, L.; Cohen, B.; Huppert, D. *J. Phys. Chem. A* **2000**, 104, 6689.
- (40) Weller, A. Z. *Phys. Chem. N. F.* **1957**, 13, 335.
- (41) Cohen, B.; Huppert, D.; Agmon, N. *J. Am. Chem. Soc.* **2000**, 122, 9838.
- (42) Robinson, R. A.; Stokes, R. H. *Electrolyte Solutions*, 2nd ed.; Butterworths: London, 1959.
- (43) Krissinel', E. B.; Agmon, N. *J. Comput. Chem.* **1996**, 17, 1085.
- (44) Flannery, M. R. *Phys. Rev. Lett.* **1981**, 47, 163.
- (45) Lee, J. *J. Am. Chem. Soc.* **1989**, 111, 427.
- (46) Agmon, N.; Huppert, D.; Masad, A.; Pines, E. *J. Phys. Chem.* **1991**, 95, 10407. Erratum, *J. Phys. Chem.* **1992**, 96, 2020.
- (47) Agmon, N.; Goldberg, S. Y.; Huppert, D. *J. Mol. Liq.* **1995**, 64, 161.
- (48) Erdey-Grüz, T. *Transport Phenomena in Aqueous Solutions*; A. Hilger: London, 1974.
- (49) Weast, R. C.; Astle, M. J., Eds.; *Handbook of Chemistry and Physics*, 66th ed.; CRC Press: Boca Raton, FL, 1985.
- (50) Sharma, L. R.; Kalia, R. K. *J. Chem. Eng. Data* **1977**, 22, 39.